magnetochemistry

MDPI

Communication

Design of Fe_7S_8@Lip Composite for the pH-Selective and Magnetically Targeted Programmed Release of H_2S

Shenghua Wang [1], Hanlin Wei [2,*], Jialian Li [2], Ning Liu [1,*], Zhiming Deng [2,*] and Junqing Huang [3,*]

[1] School of Chemical and Environmental Engineering, Hunan Institute of Technology, Hengyang 421010, China; wangshenghua0731@163.com
[2] State Key Laboratory of Chemo and Biosensing, College of Chemistry and Chemical Engineering, Hunan University, Changsha 410082, China; lijialian@hnu.edu.cn
[3] National Key Laboratory of Macromolecular Drug Development and Manufacturing, School of Pharmaceutical Science, Wenzhou Medical University, Wenzhou 325035, China
* Correspondence: hlwei@hnu.edu.cn (H.W.); liuning0731@163.com (N.L.); zhimingdeng@hnu.edu.cn (Z.D.); huangjunqing@wmu.edu.cn (J.H.)

Abstract: The significance of hydrogen sulfide (H_2S) release in vivo is multifaceted. It functions as a crucial gaseous signaling molecule with extensive physiological and pathological impacts within organisms. To create novel H_2S-releasing materials, we synthesized Fe_7S_8@Lip, a slow-release gas nanocomposite, which exhibits stable and sustained H_2S-release properties. Our gas releaser possesses selective H_2S-release capabilities, and, notably, it can achieve effective H_2S release under magnetic force with the assistance of a magnetic field. In conclusion, our findings indicate that Fe_7S_8@Lip can serve as an H_2S slow-release nanocomposite, offering a potentially innovative approach for programmed H_2S release in vivo.

Keywords: magnetically targeted; H_2S; Fe_7S_8@Lip; pH-selective

check for updates

Academic Editor: Evgeny Katz

Received: 17 January 2025
Revised: 10 March 2025
Accepted: 13 March 2025
Published: 14 March 2025

Citation: Wang, S.; Wei, H.; Li, J.; Liu, N.; Deng, Z.; Huang, J. Design of Fe_7S_8@Lip Composite for the pH-Selective and Magnetically Targeted Programmed Release of H_2S. *Magnetochemistry* **2025**, *11*, 22. https://doi.org/10.3390/magnetochemistry11030022

Copyright: © 2025 by the authors. Licensee MDPI, Basel, Switzerland. This article is an open access article distributed under the terms and conditions of the Creative Commons Attribution (CC BY) license (https://creativecommons.org/licenses/by/4.0/).

1. Introduction

The importance of H_2S (hydrogen sulfide) in organisms manifests in multiple ways [1–3]. It is not only a toxic, flammable, and corrosive gas within organisms but also a vital gaseous signaling molecule involved in regulating various physiological and pathological processes. The H_2S exerts a bidirectional regulatory effect on vascular tone, capable of both relaxing and contracting blood vessels [4–6]. Additionally, H_2S can influence the proliferation and apoptosis of vascular smooth muscle cells, as well as vascular autophagy, thereby affecting cardiovascular diseases such as atherosclerosis [7,8]. H_2S also regulates bronchial tone, participates in gas exchange within the lungs, modulates respiration, and is associated with the occurrence of diseases such as asthma, wheezing, pneumonia, and lung injury. As research on H_2S continues to deepen, scientists have discovered its broad application prospects in the medical field. For instance, the exogenous delivery of H_2S or modulation of endogenous H_2S can improve cardiac function, reduce ischemia–reperfusion injury, and mitigate heart complications in various other cardiac diseases, including arrhythmia, heart failure, myocardial hypertrophy, myocardial fibrosis, and myocardial infarction. Furthermore, H_2S-related therapeutic agents also hold promise in the treatment of neurodegenerative diseases [9]. However, there are significant challenges in delivering exogenous H_2S. Its gaseous nature leads to its very short half-life (<5 min), difficulty in targeting the lesion site, and potential cell toxicity at high doses. Although small molecule donors can slowly release H_2S, they lack tissue specificity and

may cause systemic exposure, leading to hypotension or metabolic disorders [10]. Inorganic nanocarriers (such as mesoporous silica) can load H_2S donors, but it is difficult to achieve on-demand release and their biocompatibility is questionable [11]. Therefore, it is urgent to develop a new H_2S delivery system that has targeting ability, controllable release, and high biocompatibility. Therefore, the development of novel nanoplatforms for controlled H_2S release is of significant importance for the treatment of several major diseases.

Extensive research has been conducted on the design of probes for H_2S release. For example, the Pry-Ps@CP-PEG multifunctional hydrogen sulfide nanoregulator designed by the research team can accurately locate tumor areas, achieve precise photothermal therapy, and rapidly release hydrogen sulfide to alleviate inflammation [12]. However, the majority of H_2S donors often release inadequate amounts, necessitating an increase in dosage during treatment, which subsequently heightens drug toxicity. Furthermore, the swift release kinetics of numerous H_2S donors not only hinder their prolonged therapeutic effectiveness but also pose the risk of intensifying bodily injury [13,14]. Another approach involves loading both the H_2S prodrug ADT and magnetic nanoparticles into liposomes to construct targeted controlled-release nanosystems (AMLs) for tumor-targeted therapy. This system can release H_2S at the tumor site to achieve the purpose of tumor treatment. Currently, research on nanomaterials of iron sulfide that can release hydrogen sulfide mainly focuses on Fe_3S_4 [15], which has a higher sulfur content and more complex distribution of iron valence states. This structure can obtain better catalytic activity and electrochemical capacity. In summary, although various nanomaterials capable of releasing hydrogen sulfide have been developed, they still have limitations in terms of their biocompatibility, controllability, preparation cost, targeting ability, and efficiency. Therefore, it is urgent to overcome these limitations and develop safer, more efficient, and controllable hydrogen sulfide nano-release materials.

Herein, we successfully synthesized iron sulfide (Fe_7S_8) nanoparticles with a particle size of about 16 nm using a hydrothermal method. Subsequently, these nanoparticles were further modified with liposomes to obtain a composite material with excellent bioavailability, which we named Fe_7S_8@Lip. The Fe_7S_8 nanoparticles can slowly and persistently release H_2S under weak acidic conditions, which makes them potentially valuable in biological applications. More importantly, after modification with liposomes, Fe_7S_8@Lip not only retains its original release characteristics but also acquires a magnetic guidance function. This means that, under the action of an external magnetic field, Fe_7S_8@Lip can accurately target the lesion area and release H_2S gas to respond to a weak acidic inflammatory microenvironment, thus effectively regulating the microenvironment.

2. Experimental Details

2.1. Preparation of Fe_7S_8@Lip Nanomedicine

Firstly, biodegradable Fe_7S_8 nanoparticles were prepared via a hydrothermal method [16]. A total of 1 mmoL of $FeSO_4 \cdot 7H_2O$, 1 mmol of L-Cysteine, and poly(vinyl pyrrolidone) (PVP, K30) were combined and dissolved in 30 mL of deionized (DI) water while undergoing vigorous magnetic stirring. Subsequently, 100 μL of ethylenediamine was added to the solution. The resultant mixture was then transferred to a stainless steel autoclave, sealed tightly, and heated to 200 °C for a duration of 24 h. A black precipitate was obtained through centrifugation and subsequently washed multiple times with ethanol and DI water. To encapsulate Fe_7S_8 within liposomes, thin liposomes were prepared using the thin-film hydration method [17]. Then, the thin liposomes were hydrated with Fe_7S_8 in PBS solution through vortexing and ultrasonication. The final suspension (Fe_7S_8@Lip) was further purified by centrifugation. It was then filtered through a membrane with a pore size of 0.22 μm to discard any larger residues.

2.2. Structural Characterization of Fe_7S_8@Lip Nanomedicine

The composition and structure of the nanocomposite were analyzed using Transmission Electron Microscopy (TEM), X-ray Photoelectron Spectroscopy (XPS), and Scanning Electron Microscopy (SEM). All XPS spectra were charge-corrected using the carbon contamination layer C 1s peak (binding energy of 284.8 eV). Specifically, a survey scan was collected to determine the elemental composition, followed by peak fitting of the C 1s narrow spectrum. The position of the main peak was then corrected to a standard value, and this shift was uniformly applied to the binding energy calibration of core-level spectra such as Fe 2p and S 2p. The nanoparticle size of the nanocomposite was detected using a Litesizer particle analyzer. The magnetization curves of Fe_7S_8@Lip nanoparticles were examined using a vibrating sample magnetometer (VSM) at room temperature.

2.3. Evaluation of the Performance of Releasing H_2S

The H_2S release performance was evaluated using a methylene blue standard curve. Firstly, Na_2S standard solutions with concentrations of 5, 10, 20, 40, 60, 80, and 100 μM were prepared using Na_2S and distilled water. A total of 1 mL of each concentration of Na_2S standard solution was taken, and the process was repeated three times. The reaction solution was allowed to fully react with methylene blue reagent at room temperature for 30 min. The absorption spectrum was detected using a UV-Vis spectrophotometer. Then, a standard curve was plotted for comparison. Subsequently, Fe_7S_8@Lip was mixed with 10 mL of deionized water, and 1 mL was taken each time to react with methylene blue reagent at room temperature for 30 min. The maximum absorbance was detected at 670 nm. The concentration of H_2S was calculated based on the aforementioned standard curve.

2.4. CCK-8 Assay

For the in vitro cytotoxicity assessment, the standard Cell Counting Kit-8 (CCK-8) assay was employed. Various concentrations of the Fe_7S_8@Lip nanocomposite were introduced into 96-well plates containing different populations of L02 cells at specified time points (100 μL per well). Subsequently, 10 μL of CCK-8 solution was added to each well, followed by a 1 h incubation period. The plate was then analyzed at a wavelength of 450 nm.

3. Results and Discussion

To construct a nanoplatform capable of effectively releasing H_2S, we employed a hydrothermal synthesis method to successfully prepare Fe_7S_8 nanoparticles with a uniform size and good dispersion. As shown in Figure 1A,B, these Fe_7S_8 nanoparticles had an average size of approximately 16.5 nanometers. To further enhance the biosecurity and application potential of these nanoparticles, we utilized the liposome thin-film hydration method to encapsulate the biodegradable and H_2S-releasing superparamagnetic inorganic nanomaterial, Fe_7S_8 nanoparticles, thereby creating the biosecure Fe_7S_8@Lip nanocomposite. Through characterization with Transmission Electron Microscopy (TEM), we can clearly observe that, after encapsulation with liposomes, the particle size of the nanoparticles increases to about 120 nm (Figure 1C,D). To further reveal the sulfuration reaction, X-ray diffraction (XRD, Figure S1) was performed, which matched the standard card: 24-0220. Additionally, the negative potentials (Figure S2) suggest that the successful encapsulation of liposomes occurred. This result not only further confirms the successful synthesis of liposome-encapsulated nanoparticles but also reveals the effective encapsulation of the nanoparticles by the lipid layer, providing a solid foundation for subsequent biological applications. In summary, we successfully prepared Fe_7S_8@Lip nanocomposites with a hydrogen sulfide release functionality. This material not only possesses a uniform nanopar-

ticle size and good dispersion but also achieves enhanced biosecurity through liposome encapsulation, providing powerful support for subsequent biological experiments and medical applications.

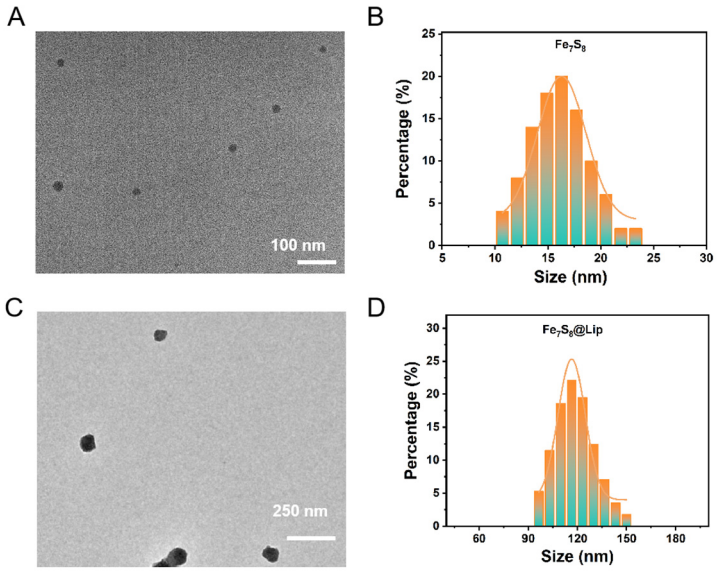

Figure 1. (**A**,**B**) TEM image of Fe_7S_8 nanoparticles and their corresponding size distribution. (**C**,**D**) TEM image of Fe_7S_8@Lip nanocomposites and their corresponding size distribution.

The valence states of Fe and S were analyzed via X-ray electron spectroscopy (XPS). Typical Fe and S peaks were detected in the full-scan XPS spectrum (Figure 2A). In the Fe 2p region, two peaks at 707.6 eV and 710.3 eV were assigned to Fe(ii). The Fe peak at $2p_{3/2}$ = 720.2 eV can be assigned to Fe0. The binding energies of Fe $2p_{3/2}$ and Fe $2p_{1/2}$ were 713.3 eV and 724.4 eV, respectively, proving the existence of Fe(iii) (Figure 2B). As shown in Figure 2C, the binding energies observed at 161.08 eV and 162.18 eV correspond to S^{2-} 2p3/2 and 2p1/2, respectively, which suggests that Fe7S8 NPs contain sulfur, allowing for the release of H_2S. At the same time, during our comprehensive analysis, we also distinctly detected the presence of signals corresponding to the elements C, H, and O. These signals are predominantly attributed to the unique modification of iron sulfide that was carried out through the utilization of liposomes, indicating the successful integration of these components within the experimental setup (Figure 2D–F).

As shown in Figure 3A, before the application of a magnet, the nanoparticles exhibit a uniform dispersion state, being scattered irregularly in the solution, and are independent and do not interfere with each other. However, when the magnet is introduced and allowed to adsorb for 60 s, these nanoparticles begin to move in an orderly manner towards the side where the magnet is placed under the action of the small magnetic field, and eventually uniformly adsorb on that side, forming a dense layer of nanoparticles. It is noteworthy that the magnetic saturation value of these nanoparticles reaches up to 10 emu/g (Figure 3B), a figure that strongly demonstrates their superparamagnetic properties. This implies that, under the influence of an external magnetic field, these nanoparticles can rapidly respond and adjust their magnetization state, exhibiting strong magnetism and magnetic responsiveness. This superparamagnetism not only facilitates the manipulation of nanoparticles in magnetic fields but also opens up new possibilities for their application in fields such as biomedicine and materials science.

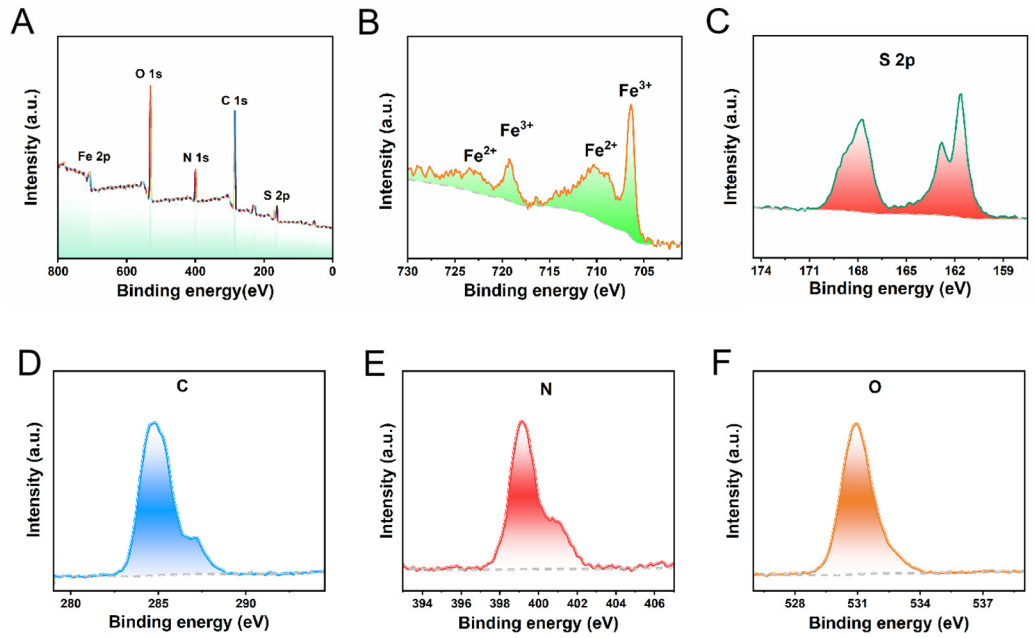

Figure 2. XPS of Fe_7S_8: (**A**) survey spectra, (**B**) Fe spectra, (**C**) S spectra, and (**D**–**F**) C, N, and O spectra.

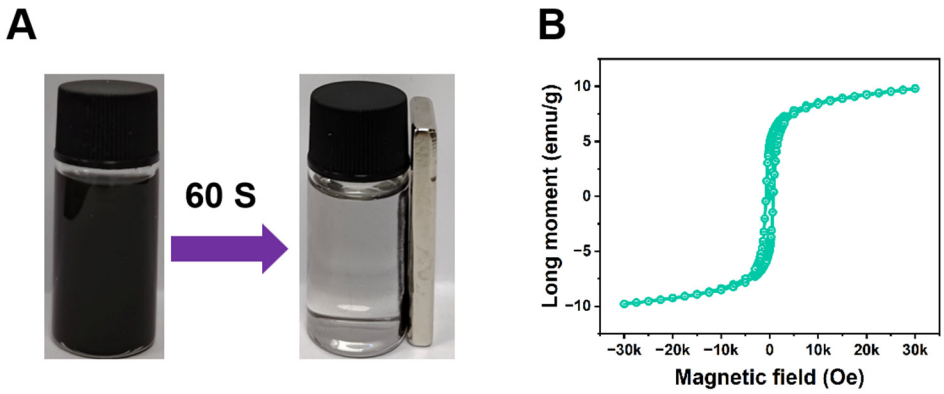

Figure 3. (**A**) Digital photos of Fe_7S_8 before and after magnetic action. (**B**) Hysteresis (M-H) analysis of Fe_7S_8.

Certain disease tissues create an environment with a reduced pH level, presenting a weakly acidic condition. Therefore, we investigated the H_2S release from Fe_7S_8@Lip nanocomposites in solutions of different pH values. The results indicate that Fe_7S_8@Lip nanocomposites release more H_2S under acidic conditions (as shown in Figure 4A). The main mechanism of this is that sulfur in Fe_7S_8 exists in the form of sulfide ions. In an acidic environment, H^+ undergoes a protonation reaction with sulfides to generate volatile gas H_2S. Consequently, the Fe_7S_8@Lip nanocomposites can serve as effective slow-release gas reactors with the ability to efficiently scavenge reactive oxygen species (ROS) and reactive nitrogen species (RNS). For in vivo applications, materials with good blood biocompatibility are fundamental and crucial. To assess the blood biocompatibility of the nanomaterial, we conducted hemolysis tests. The test results show that the nanomaterial exhibits excellent blood compatibility (Figure 4B), with a hemolysis rate below 5% at a concentration of 200 μg/mL, which is a very desirable indicator. Further observation reveals that the structure of red blood cells remained intact during this process, further confirming the good biocompatibility of the nanomaterial. Based on these test results, to ensure the safety and effectiveness of the experiments, we strictly stipulated in subsequent in vivo experiments that the maximum concentration of nanoprobes in mouse blood must be strictly controlled

below 200 μg/mL. This concentration setting aims to fully safeguard the life and health of the experimental mice while ensuring that the nanoprobes can achieve the best detection effect in vivo. Additionally, we tested the toxicity of the nanomaterial using the CCK8 assay (Figure 4C). The CCK8 test results showed that as the material concentration increased, the cell survival rate remained stable, proving that our designed material, after being encapsulated with liposomes, exhibits excellent biocompatibility, which provides an opportunity for the subsequent delivery of hydrogen sulfide to deep tissues in living organisms.

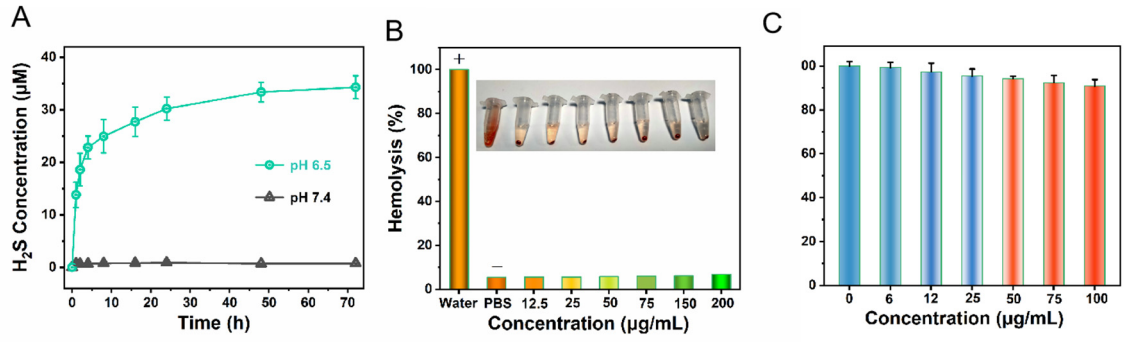

Figure 4. (**A**) H_2S release efficiency of Fe_7S_8@Lip nanocomposites in different pH environments. (**B**) Hemolysis experiment of Fe_7S_8@Lip nanocomposites. (**C**) Cell toxicity experiment of Fe_7S_8@Lip nanocomposites.

4. Conclusions

Herein, we designed a nanoplatform capable of H_2S release. The gas releaser we designed possesses the ability to selectively release H_2S based on pH levels. Notably, with the assistance of a magnetic field, it can achieve efficient H_2S release through magnetic force. Furthermore, when encapsulated in liposomes, the nanoprobes exhibit excellent biocompatibility. In conclusion, our findings suggest that Fe_7S_8@Lip can serve as an H_2S slow-release nanocomposites, offering a potentially innovative approach to programmed H_2S release in the deep tissues of living organisms and the detection and treatment of major diseases.

Supplementary Materials: The following supporting information can be downloaded at: https://www.mdpi.com/article/10.3390/magnetochemistry11030022/s1, Figure S1: The XRD of Fe_7S_8; Figure S2: Zeta potential of Fe_7S_8 and Fe_7S_8@Lip nanoparticles.

Author Contributions: Formal analysis, J.L. and N.L.; Data curation, H.W. and J.H.; Writing—original draft, S.W.; Writing—review & editing, Z.D.; Funding acquisition, N.L. All authors have read and agreed to the published version of the manuscript.

Funding: This work was supported by the Research Foundation of Education Bureau of Hunan Province, China (22A0628), Natural Science Foundation of Hunan Province (2025JJ70140) and China Postdoctoral Science Foundation (2023M731063).

Data Availability Statement: The data used to support the findings of this study are included within the article.

Conflicts of Interest: The authors declare no competing financial interests.

References

1. Shaik, R.; Kishore, R.; Kumar, A.; Shekhar, C.; Kumar, M. Metal oxide nanofibers based chemiresistive H_2S gas sensors. *Coord. Chem. Rev.* **2022**, *471*, 214752. [CrossRef]
2. Zhao, Z.N.; Guo, W.Y.; Xu, C.W.; Wang, Q.; Mao, C.; Wan, M.M. Physiological functions and donor design of hydrogen sulffde and its application in central nervous system diseases. *Chem. Eng. J.* **2023**, *452*, 139089. [CrossRef]

3. Kimura, H. Signaling by hydrogen sulffde (H_2S) and polysulffdes (H_2S_n) in the central nervous system. *Neurochem. Int.* **2019**, *126*, 118–125. [CrossRef] [PubMed]
4. Sun, L.H.; Wu, Y.L.; Chen, J.J.; Zhong, J.; Zeng, F.; Wu, S.Z. A Turn-On Optoacoustic Probe for Imaging Metformin-Induced Upregulation of Hepatic Hydrogen Sulfide and Subsequent Liver Injury. *Theranostics* **2019**, *9*, 77–89. [CrossRef] [PubMed]
5. Kabil, O.; Banerjee, R. Enzymology of H_2S Biogenesis, Decay and Signaling. *Antioxid. Redox Signal.* **2014**, *20*, 770–782. [CrossRef] [PubMed]
6. Yang, G.; Wu, L.; Jiang, B.; Yang, W.; Qi, J.; Cao, K. H_2S as a Physiologic Vasorelaxant: Hypertension in Mice with Deletion of Cystathionine γ-Lyase. *Science* **2008**, *322*, 587–590. [CrossRef] [PubMed]
7. Abe, K.; Kimura, H. The Possible Role of Hydrogen Sulfide as an Endogenous Neuromodulator. *J. Neurosci.* **1996**, *16*, 1066–1071. [CrossRef] [PubMed]
8. Wiliński, B.; Wiliński, J.; Somogyi, E.; Piotrowska, J.; Opoka, W. Metformin Raises Hydrogen Sulfide Tissue Concentrations in Various Mouse Organs. *Pharmacol. Rep.* **2013**, *65*, 737–742. [CrossRef]
9. Zhou, L.N.; Wang, Q. Advances of H_2S in Regulating Neurodegenerative Diseases by Preserving Mitochondria Function. *Antioxidants* **2023**, *12*, 652. [CrossRef] [PubMed]
10. Ranjana, M.; Kulkarni, R.M.; Sunil, D. Small Molecule Optical Probes for Detection of H_2S in Water Samples: A Review. *ACS Omega* **2024**, *9*, 14672–14691.
11. Bulemo, P.M.; Cho, H.J.; Kim, N.H.; Kim, I.D. Mesoporous SnO_2 Nanotubes via Electrospinning–Etching Route: Highly Sensitive and Selective Detection of H_2S Molecule. *ACS Appl. Mater. Interfaces* **2017**, *9*, 26304–26313. [CrossRef] [PubMed]
12. Li, J.; Xie, L.S.; Li, B.; Yin, C.; Wang, G.H.; Sang, W.; Li, W.X.; Tian, H.; Zhang, Z.; Zhang, X.J.; et al. Engineering a Hydrogen-Sulfide-Based Nanomodulator to Normalize Hyperactive Photothermal Immunogenicity for Combination Cancer Therapy. *Adv. Mater.* **2021**, *33*, 2008481. [CrossRef] [PubMed]
13. He, Q.J. Precision gas therapy using intelligent nanomedicine. *Biomater. Sci.* **2017**, *5*, 2226–2230. [CrossRef] [PubMed]
14. Ding, H.; Chang, J.H.; He, F.; Gai, S.L.; Yang, P.P. Hydrogen sulffde: An emerging precision strategy for gas therapy. *Adv. Healthc. Mater.* **2022**, *11*, 2101984. [CrossRef] [PubMed]
15. Liu, J.; Guo, X.; Zhao, Z.; Li, B.; Qin, J.; Peng, Z.; He, G.; Brett, D.J.; Wang, R.; Lu, X. Fe7S8 nanoparticles for arterial inflammation therapy: Integration of magnetic hyperthermia and photothermal treatment. *Appl. Mater. Today* **2020**, *18*, 100457. [CrossRef]
16. Shi, Y.B.; Wang, X.B.; Liu, X.F.; Ling, C.C.; Shen, W.J.; Zhang, L.Z. Visible light promoted Fe_3S_4 Fenton oxidation of atrazine. *Appl. Catal. B Environ.* **2020**, *277*, 119229. [CrossRef]
17. Thabet, Y.; Elsabahy, M.; Eissa, N.G. Methods for preparation of niosomes: A focus on thin-film hydration method. *Methods* **2022**, *199*, 9–15. [CrossRef] [PubMed]

Disclaimer/Publisher's Note: The statements, opinions and data contained in all publications are solely those of the individual author(s) and contributor(s) and not of MDPI and/or the editor(s). MDPI and/or the editor(s) disclaim responsibility for any injury to people or property resulting from any ideas, methods, instructions or products referred to in the content.